

A CONSISTENT ONE-DIMENSIONAL MODEL FOR THE TURBULENT TACHOCLINE

K. Petrovay

*Eötvös University, Dept. of Astronomy, Budapest, Pf. 32, H-1518 Hungary
and*

*Center for Turbulence Research, NASA Ames Research Center, Moffett Field,
California 94035*

[*Solar Physics*, submitted]

Abstract.

The first consistent model for the turbulent tachocline is presented, with the turbulent diffusivity computed within the model instead of being specified arbitrarily. For the origin of the 3D turbulence a new mechanism is proposed. Owing to the strongly stable stratification, the mean radial shear is stable, while the horizontal shear is expected to drive predominantly horizontal, quasi-2D motions in thin slabs. Here I suggest that a major source of 3D overturning turbulent motions in the tachocline is the *secondary shear instability* due to the strong, random vertical shear arising between the uncorrelated horizontal flows in neighbouring slabs. A formula for the vertical diffusivity due to this turbulence, equation (9), is derived and applied in a simplified 1D model of the tachocline. It is found that Maxwell stresses due to an oscillatory poloidal magnetic field of a few hundred gauss are able to confine the tachocline to a thickness below 5 Mm. The integral scale of the 3D overturning turbulence is the buoyancy scale, on the order of 10 km and its velocity amplitude is a few m/s, yielding a vertical turbulent diffusivity on the order of $10^8 \text{ cm}^2/\text{s}$.

Keywords: Sun: interior, MHD, tachocline

1. Introduction

In most current dynamo models (see e.g. Petrovay, 2000, for a review), the strong toroidal magnetic field responsible for solar activity is generated in the thin rotational shear layer below the convective zone (CZ), known as the tachocline. To hold sufficient magnetic flux to explain the flux observed at the surface without unrealistically high field strengths, this layer should be at least a few megameters thick. On the other hand, a magnetic field oscillating with a circular frequency $\omega_{\text{cyc}} = 2\pi/P$, ($P = 22$ years is the solar cycle period) is known to penetrate a conductive medium only down to a skin depth of

$$H_{\text{skin}} = (2\eta/\omega_{\text{cyc}})^{1/2} \quad (1)$$

where η is the magnetic diffusivity. If $H_{\text{skin}} > 1 \text{ Mm}$ then we conclude from this that for present-day dynamo models to work, we must have



© 2003 Kluwer Academic Publishers. Printed in the Netherlands.

$\eta \gtrsim 10^8 \text{ cm}^2/\text{s}$ in the tachocline layer. For comparison, the molecular magnetic diffusivity is $\sim 10^3 \text{ cm}^2/\text{s}$ in this part of the Sun, while the turbulent diffusivity in the convective zone is estimated to be 10^{12} – $10^{13} \text{ cm}^2/\text{s}$.

Helioseismic evidence indicates that at low heliographic latitudes the middle of the tachocline is situated at $0.69 R_\odot$ ($1 R_\odot = 698 \text{ Mm}$ is the solar radius) and its thickness is less than a few percent of R_\odot (Kosovichev, 1996). There are indications that at high latitudes the tachocline is situated at slightly shallower depths, $r = 0.705 R_\odot$, and it may also be marginally thicker (Basu and Antia, 2001). Comparing this with the radius of the bottom of the adiabatically stratified convective zone, $0.71 R_\odot$, it is clear that most of the tachocline lies in the radiative interior, especially near the equator, so the relatively high value of the (presumably turbulent) magnetic diffusivity inferred above is puzzling. Hence, there is clearly a need to understand the nature of small-scale turbulent motions in the tachocline. Unfortunately, while the thermal stratification in the tachocline is relatively well known, its fluid dynamical properties, including the precise profile of the rotational flow $v(r, \theta)$, the meridional flow, and the characteristics of turbulence, are very poorly constrained by observations.

The tachocline is thus basically an MHD shear flow in the azimuthal direction in a thin, rotating spherical shell with both radial and latitudinal shear and a strongly stable stratification (Richardson number $\sim 10^3$). Theoretical understanding and experimental knowledge regarding turbulence in stratified shear flows has been reviewed by Hopfinger (1987) and Thorpe (1987). These reviews emphasize the tendency towards two-dimensional, predominantly horizontal motions in such situations, the vertical motions being limited to the small *buoyancy scale* (see below). In line with the concepts outlined in those reviews, the present paper relies on theoretical arguments concerning the properties of turbulent motions in such conditions. On the basis of such arguments, simplified one- or two-dimensional models may be constructed for the mean flow, or appropriate subgrid closure schemes may be constructed for full 3D large-eddy simulations. While such arguments have been attempted in the past (Spiegel and Zahn, 1992, Gough and McIntyre, 1998), in the lack of detailed turbulence calculations to be used for subgrid closures, all tachocline models published to date have either simply ignored turbulence (Rüdiger and Kitchatinov, 1997, MacGregor and Charbonneau, 1999, Garaud, 2001a, Cally, 2001), or assumed arbitrary fixed scalar turbulent diffusivities in 2D mean flow models (Forgács-Dajka and Petrovay, 2001, 2002, Forgács-Dajka, 2003) and in 3D LES (Miesch, 2001, 2002).

The aim of the present work is to attempt to remedy this situation by considering, on the basis of the known stability criteria, the possible sources of turbulence in a strongly stably stratified shear flow with both vertical and horizontal shear, and discussing the expected properties of the turbulence generated by it, on the basis of a dimensional analysis of the K - ϵ equations. As our analysis does not consider the effects of spherical geometry, rotation, meridional circulation, non-adiabatic convective overshoot, or magnetic instabilities, it should only be regarded as a first step towards a more comprehensive theoretical analysis of the problem of turbulence in the solar tachocline. These theoretical arguments can be found in Section 2. Then, in Section 3, as an illustration of the use of such theoretical considerations, our prescription for calculating the turbulent diffusivity in the tachocline, equation (9), is incorporated in a simplified one-dimensional model for the tachocline. The results show that Maxwell stresses due to an oscillatory poloidal magnetic field of a few hundred gauss (a rather moderate value) are able to confine the tachocline to a thickness below 5 megameters. The conditions of validity of our treatment are discussed in Section 4. Finally, Section 5 concludes the paper by comparing our suggested picture of tachocline turbulence with numerical simulation results and discussing the implications of the results.

2. A possible source of turbulence: the secondary shear instability

The thermal stratification of the Sun is quite accurately known from a comparison of standard solar models with helioseismic inversion results. The radiative interior below the CZ is characterized by significant negative values of $\Delta\nabla$. For rough estimates, a useful approximation in the tachocline region (i.e. near the top of the radiative zone) is $\Delta\nabla \sim -0.015 z$ [Mm], where $z = r_{bcz} - r$ is the depth below the bottom of the convective zone, at a radius value of $r_{bcz} = 0.71R_\odot$. On the other hand, the pressure scale height in this region is $H_P = -P dz/dP \sim 50$ Mm. With $g = 5 \cdot 10^4$ cm²/s, this yields a Brunt-Väisälä frequency

$$N_{BV}^2 [\text{s}^{-2}] = -\Delta\nabla g / H_P \sim 1.5 \cdot 10^{-7} z [\text{Mm}], \quad (2)$$

i.e. at a depth of a few megameters $N_{BV} \sim 10^{-3}$ s⁻¹.

A displaced mass element will then oscillate around its equilibrium position under the action of buoyancy on a timescale $N_{BV}^{-1} \sim 10^3$ s. The amplitude of the oscillation is clearly $\sim v_z/N_{BV}$, so in the presence of turbulent motions, these motions will be limited to a vertical scale $l_b = K^{1/2}/N_{BV}$, called the *buoyancy scale*. ($K = \overline{v_z^2}$ is the kinetic

energy in the vertical component of motions.) On the other hand, as an elementary estimate gives $\nu \sim K^2/\epsilon$ for the vertical turbulent diffusivity, one has $l_b \sim (\nu/N_{BV})^{1/2}$. Vertical overturning motions on scales exceeding l_b will be strongly damped by gravity wave emission.

The pole-equator difference in the rotational rate of the convective zone is about 30% of the equatorial rotation rate. Taking half of this value to be the characteristic amplitude of the differential rotation (cf. eq. (5) below), we have a differential rotation amplitude $\Delta v_0 \sim 3 \cdot 10^4$ cm/s at the top of the tachocline. This value is clearly also roughly the amplitude of the vertical velocity difference across the tachocline, so the characteristic vertical shear is

$$S \sim \Delta v_0 / H \sim 3 \cdot 10^{-5} \text{ s}^{-1} \quad (3)$$

where H is the scale height of Δv , as given by equation (5) below. Helioseismic calibrations (Basu and Antia, 2001) indicate $H \sim 10$ Mm. This yields a Richardson number $\text{Ri} = N_{BV}^2 / S^2 \sim 10^3$. This enormous value shows that the vertical shear cannot directly drive turbulence in the tachocline.

Buoyancy, however, cannot stabilize the horizontal shear. While linear stability analysis (Dziembowski and Kosovichev, 1987, Charbonneau, Dikpati, and Gilman, 1999) shows that the horizontal shear is close to marginal stability in the 2D nonmagnetic case, nonlinear, 3D effects and magnetic fields are known to lead to strong instability (Gilman and Dikpati, 2000, Dikpati and Gilman, 2001). The motions driven by the horizontal shear instability are predominantly horizontal, and their spatial scale is

$$l_h \sim R_\odot, \quad (4)$$

On the basis of general experience with shear flow turbulence¹, the velocity scale v_h of the horizontal motions driven by the shear instability may be assumed to be close to the amplitude Δv of the horizontal shear at the given depth:

$$v_h \sim \Delta v = [\omega(z, \theta = 0) - \omega(z, \theta = \pi/2)]R_\odot/2 \quad (5)$$

Similarly, their correlation time is assumed to be

$$l_h/v_h \sim R_\odot/\Delta v \quad (6)$$

OVERTURNING TURBULENT MOTIONS IN THE VERTICAL DIRECTION ARE IMPEDED BY THE STABLE STRATIFICATION, THEIR SCALE BEING LIMITED TO l_b . OWING TO THE

¹ In fact it is not obvious that this experience is a useful guide under conditions in the solar tachocline. This point will be discussed further in Sect. 4 below.

low vertical diffusivity and the finite correlation time, the horizontal motions will be characterized by a limited vertical correlation length

$$l_c \sim (\nu l_h / v_h)^{1/2}. \quad (7)$$

The random horizontal flows driven by the shear will then be limited to thin sheets of thickness l_c , the motion in neighbouring sheets being independent. This will give rise to random vertical shear between neighbouring sheets, of amplitude

$$S_2 \sim v_h / l_c \sim (v_h^3 / \nu l_h)^{1/2} \quad (8)$$

This *secondary vertical shear* is much stronger than the primary (mean) vertical shear, the corresponding Richardson number being

$$Ri_2 = g \Delta \nabla \nu l_h / H_P v_h^3.$$

Substituting here the characteristic values of the parameters, we find that $Ri_2 < 0.25$, i.e. the secondary shear is unstable, if

$$\nu < \nu_{cr} = \frac{v_h^3}{4l_h N_{BV}^2} \simeq 10^{-4} \frac{v_h^3 [\text{CGS}]}{z [\text{Mm}]} \quad (9)$$

In a depth of a few megameters this value is $\nu_{cr} \sim 10^8 \text{ cm}^2/\text{s}$, much higher than the molecular value, so we expect that, in the absence of other sources of turbulence, the secondary shear is strongly unstable.

What is the characteristic amplitude of the turbulent motions driven by the secondary shear instability? In principle, this could be derived from a $K-\epsilon$ model (or, more, generally, from a Reynolds stress model (Speziale, 1991). Assuming plane parallel geometry for simplicity, the relevant equations are of the general form

$$\frac{\partial K}{\partial t} = P_K - D_K - \frac{\partial F_K}{\partial z} \quad (10)$$

$$\frac{\partial \epsilon}{\partial t} = P_\epsilon - D_\epsilon - \frac{\partial F_\epsilon}{\partial z} \quad (11)$$

Here, the non-local fluxes or third order moments are

$$F_K = \overline{v_z^3} \quad (12)$$

$$F_\epsilon = \overline{v_z \epsilon_l} \quad (13)$$

ϵ_l being the local dissipation rate, while ϵ is the mean dissipation. The production terms are usually modelled as

$$P_K = \frac{\nu}{2} S_2^2 \quad (14)$$

$$P_\epsilon = C_P \frac{\epsilon}{K} P_K \quad (15)$$

while, assuming an ideal gas and the Boussinesq approximation $\rho'/\rho = -T'/T$ (prime denotes fluctuations), the dissipation/sink terms read

$$D_K = \epsilon + g \overline{v_z T'} \quad (16)$$

$$D_\epsilon = C_{D1} \frac{\epsilon^2}{K} + C_{D2} \frac{\epsilon}{K} g \overline{v_z T'} \quad (17)$$

(The first terms on the r.h.s. represent viscous dissipation, while the second terms correspond to gravity wave emission. Note that in a subadiabatic environment $\overline{v_z T'} > 0$, i.e. downmoving fluid parcels are hotter than average.)

Performing a dimensional analysis on these equations we find that the diffusive timescale, corresponding to the non-local terms, is $d^2/\nu \gtrsim d^2/\nu_{\text{cr}} \sim 10^{10}$ s, while the timescale associated with the shear production term is $K/\nu S_2^2 \sim N_{\text{BV}}/S_2^2 \sim N_{\text{BV}} l_h \nu / v_h^3 \sim 10^{-5} \nu < 10^3$ s. This implies that the transport terms can be neglected in the K - ϵ equations. Under such conditions the equations have no stationary solution, as the values of the constants C_P , C_{D1} and C_{D2} are different in general. The intensity of turbulence will then keep increasing until the turbulent diffusivity reaches the critical value ν_{cr} , when further shear production is switched off.

We thus conclude that the secondary vertical shear instability can be expected to drive overturning turbulence to the level $\nu = \nu_{\text{cr}}$ on a short timescale. The turbulence generated by this mechanism may then be crudely represented by the vertical diffusivity value given by eq. (9).

3. Tachocline model

3.1. MODEL EQUATIONS

We now proceed to develop a simple one-dimensional model for the solar tachocline, assuming that the secondary shear instability discussed in the previous section is the only source of turbulence in the tachocline region. Our computational domain will be restricted to the top of the radiative interior, below r_{bcz} .

The convective zone is characterized by extremely high turbulent diffusivities. Due to the Coriolis force, the Reynolds stress tensor also has significant nondiagonal components in the convective envelope. These components imply an angular momentum transport which is thought to be the main driver of solar differential rotation. Based on the discussion of the previous section we expect that the amplitude

of turbulence in the tachocline is much lower than in the CZ. Thus, from the point of view of tachocline modelling, it is not unrealistic to regard the latitudinal differential rotation at $r = r_{bcz}$ as a given boundary condition imposed at the top of the region of interest. This is tantamount to assuming that differential rotation is driven by a highly effective mechanism in the convective zone which is not seriously influenced by the processes in the tachocline.

As the layer studied is thin, we also adopt a plane parallel representation for it, with constant density. (The effects of the stable density stratification are only implicitly taken into account by its role in determining the turbulent viscosity, eq. (9).)

Thus, we regard the following model problem. Consider a plane parallel layer of incompressible fluid of density ρ , where the viscosity ν and the magnetic diffusivity η depend on z only. At $z = 0$ where z is the vertical coordinate (corresponding to depth in the solar application we have in mind) a periodic horizontal shearing flow is imposed in the y direction:

$$v_{y0} = v_0 \cos(kx)$$

(so that x will correspond to heliographic latitude, while y to the longitude). We assume a two-dimensional flow pattern ($\partial/\partial y = 0$) and $v_x = v_z = 0$ (no “meridional flow”). An oscillatory horizontal “poloidal” field is present in the x direction, given by

$$V_p = \frac{1}{(4\pi\rho)^{1/2}} \frac{\partial A}{\partial z} \quad (18)$$

(in Alfvénic units). The “toroidal” (i.e. y) component A of the vector potential obeys the corresponding component of the integral of the induction equation, which in our case simplifies to a diffusion equation:

$$\frac{\partial A}{\partial t} = \frac{\partial}{\partial z} \left(\eta \frac{\partial A}{\partial z} \right) \quad (19)$$

The upper boundary condition is $A = A_0 \cos(\omega t)$ at $z = 0$, where A_0 fixes the poloidal field amplitude.

The evolution of the azimuthal components of the velocity and the magnetic field is described by the corresponding components of the equations of motion and induction, respectively. Introducing $v = v_y$ and using Alfvén speed units also for the toroidal magnetic field

$$b = B_y (4\pi\rho)^{-1/2}, \quad (20)$$

these can be written as

$$\frac{\partial v}{\partial t} = V_p \cos(\omega t) \frac{\partial b}{\partial x} + \frac{\partial}{\partial z} \left(\nu \frac{\partial v}{\partial z} \right) \quad (21)$$

$$\frac{\partial b}{\partial t} = V_p \cos(\omega t) \frac{\partial v}{\partial x} + \frac{\partial}{\partial z} \left(\eta \frac{\partial b}{\partial z} \right) \quad (22)$$

where we have taken into account that, owing to the thinness of the tachocline, the vertical derivatives dominate the diffusive terms.² As the imposed poloidal field V_p is independent of x , Fourier transforming (21) and (22) in terms of x yields the same equations for the Fourier amplitudes \hat{v} and \hat{b} , except that $\partial/\partial x$ is substituted by ik :

$$\frac{\partial v}{\partial t} = ikbV_p \cos(\omega t) + \frac{\partial}{\partial z} \left(\nu \frac{\partial v}{\partial z} \right) \quad (23)$$

$$\frac{\partial b}{\partial t} = ikvV_p \cos(\omega t) + \frac{\partial}{\partial z} \left(\eta \frac{\partial b}{\partial z} \right) \quad (24)$$

(Hats are omitted to simplify notation.) For a rough estimate, we write $\pi b/P$ for the l.h.s. of (24), then substitute the resulting expression of b into (23), take the real part, and omit the factor $\cos^2(\omega t)$ in the first term on the r.h.s.:

$$\frac{\partial v}{\partial t} = -k^2 V_p^2 P v + \frac{\partial}{\partial z} \left(\nu \frac{\partial v}{\partial z} \right) \quad (25)$$

The equations to solve are thus (18), (19) and (25), with the turbulent diffusivities $\nu = \eta = \nu_m + \nu_{\text{cr}}$ given by equation (9) with the identification $v_h = v$. ν_m is a minimal diffusivity value (“molecular diffusivity”).

The simplified form of the first term in equation (25) will not allow a correct reproduction of the periodic part of the time dependence. The important point is, however, that this sink term, representing the reduction of horizontal shear by Maxwell stresses, has the right amplitude and the correct scaling with V_p , P , v , and k , so it may be expected to reproduce well the cycle-averaged flow amplitude as a function of z , which is our main interest here. Indeed, solving our equations for the case of constant diffusivities ν and η , the results are in a remarkably good agreement with the full 2D solutions in spherical geometry, presented in Forgács-Dajka and Petrovay (2002).

The equations were solved numerically by a finite difference scheme second-order accurate in time. All quantities were set to zero at the lower boundary, situated at $z_0 = 60$ or 30 Mm below r_{bcz} , while the boundary conditions applied at top ($z = 0$) were $v = v_0 = 3 \cdot 10^4$ cm/s and different prescribed values for A_0 . As equation (9) is singular at $z = 0$, ν was set to a high finite value ν_{max} here. For ν_m we used

² The large-scale quasi-2D motions are assumed not to contribute to angular momentum transport here, as the amplitude and sense of such a contribution is still highly controversial, cf. Spiegel and Zahn (1992), Gough and McIntyre (1998).

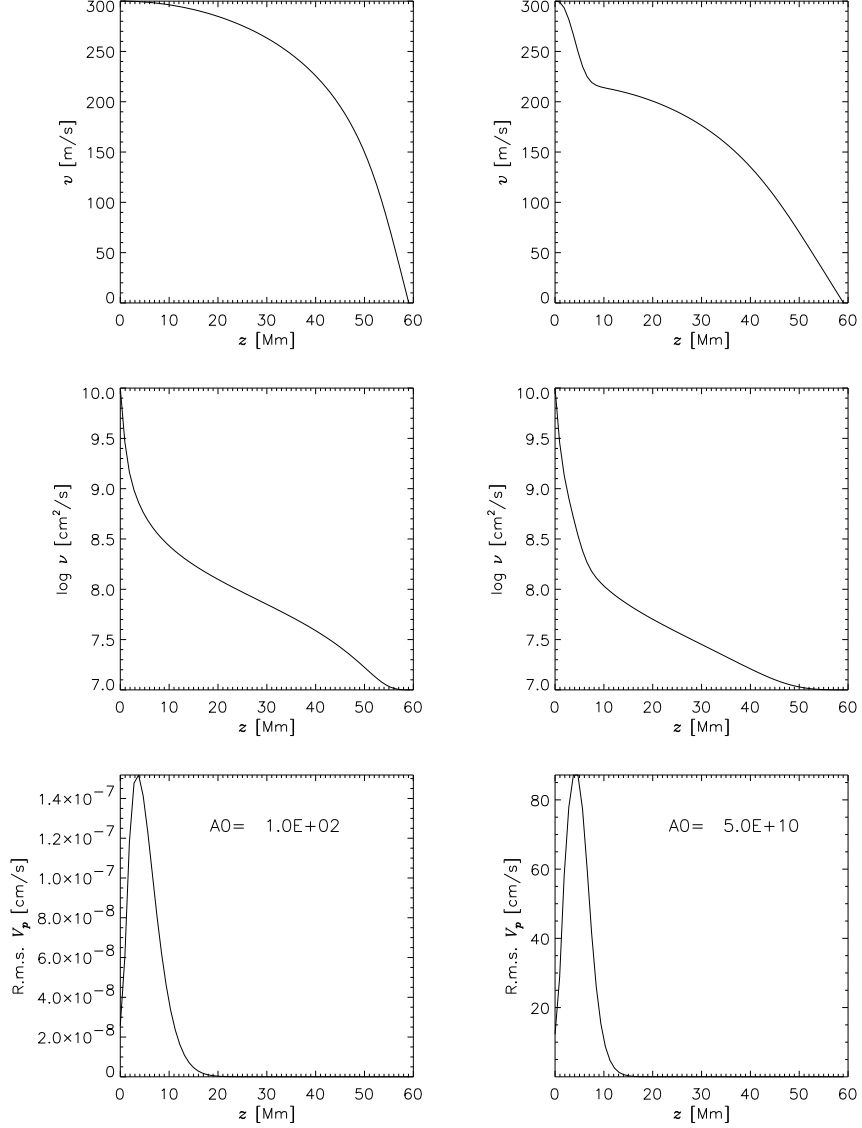


Figure 1. Horizontal differential rotation amplitude $v = v_h$, as defined in eq. (5) (top row), vertical turbulent diffusivity ν (middle row), and poloidal magnetic field in Alfvénic units (bottom row), averaged over a solar half-cycle, as functions of depth below the convective zone, for a very low (left-hand column) and a medium (right-hand column) value of the field strength imposed at the top. Note that by coincidence, in the solar tachocline the field strength in gauss is roughly equal to the corresponding Alfvén speed in cm/s.

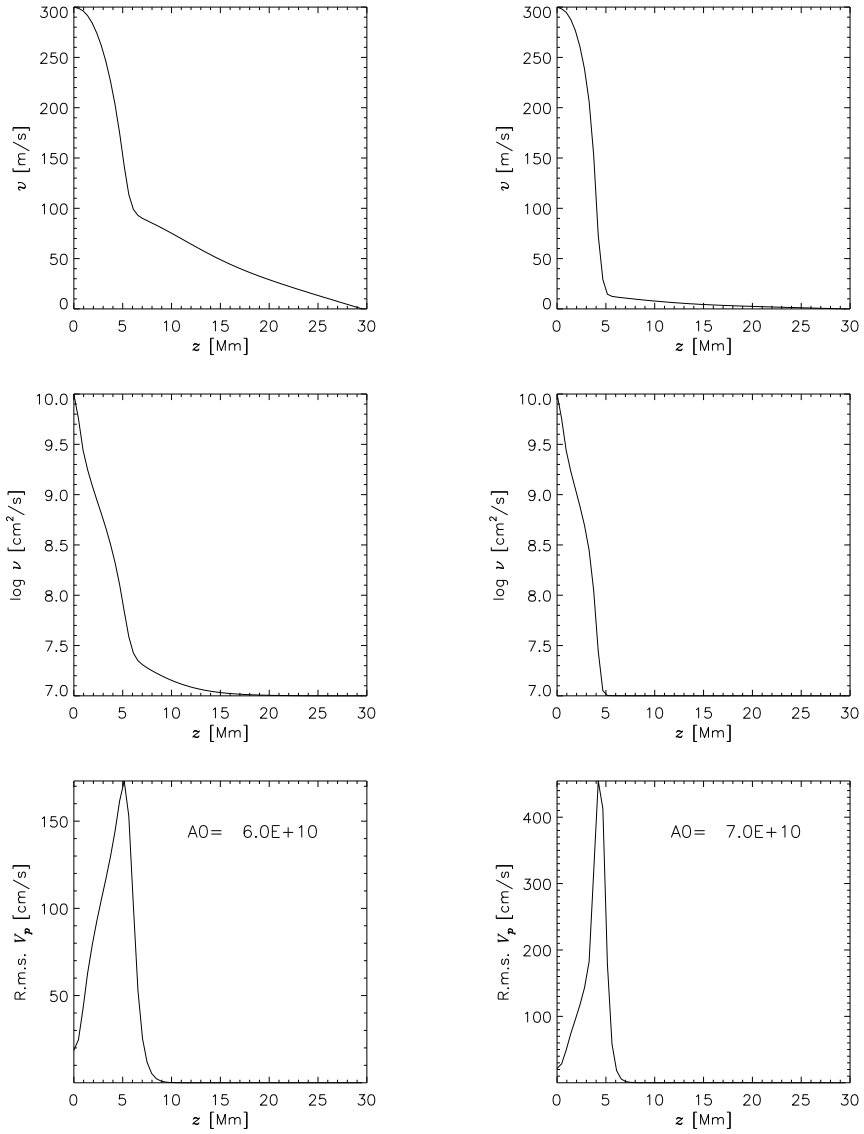


Figure 2. Same as Fig. 1 for two higher field strength values.

the value 10^7 cm²/s. This is much higher than the actual molecular diffusivities in the tachocline, but using a realistic value would lead to forbiddingly long integration times. Similarly, a too high value for ν_{\max} would lead to very short timesteps, also increasing the computing time to unaffordable values. Test runs with varying values of ν_{\max} and ν_m , however, show that these choices do not significantly distort the results.

Starting from an arbitrary initial state, the system was allowed to evolve until very nearly periodic behaviour sets in (in about 10^4 years, depending on the value of ν_m), then average quantities for one 11-year half-cycle were computed and plotted as functions of depth (Figs. 1 and 2).

3.2. RESULTS

In the case with a very weak magnetic field (left-hand column in Fig. 1), it is straightforward to show that equation (25) with ν given by (9) admits the analytic solution

$$v = v_0 \left[1 - \left(\frac{z}{z_0} \right)^2 \right]^{1/4}, \quad (26)$$

confirmed by the numerical calculations. This essentially means that in this case the shear penetrates as far down into the radiative interior as the placement of the lower boundary condition allows. The weak magnetic field itself only penetrates down to the skin depth given by equation (1), as expected. It is worth noting that the poloidal field amplitude shows a non-monotonic behaviour with depth in all cases, reaching its maximum at some finite z value. This is due to the variable diffusivity: the horizontal field lines tend to “pile up” where the diffusivity is significantly reduced.

From the right-hand column of Fig. 2 we can see that a poloidal magnetic field of a few hundred gauss (peak strength 500 G) can confine the tachocline to a thickness of barely 5 Mm.

One might think that an intermediate field strength might lead to a somewhat thicker tachocline. This is, however, not the case: an inspection of the full series of results in our figures clearly shows that a weaker field simply results in an “aborted tachocline”, i.e. the horizontal shear is first reduced by a factor depending on the field strength in a thin layer of a few Mm, but below that layer, as the magnetic field is damped by the skin effect, it follows the field-free solution (26), with a lower amplitude.

4. Discussion: conditions of validity

4.1. SCALES OF THE HORIZONTAL MOTIONS

One important assumption in our model was that the velocity and time scales of horizontal motions due to the shear instability are given by equations (5) and (6). This is indeed the general experience with unstable shear flows, its physical background being an equilibrium between growth and turbulent dissipation of the dominant modes. The growth timescale is

$$\tau_g \sim l_h/\Delta v \quad (27)$$

while the dissipation timescale is

$$\tau_d \sim l_h^2/\nu_h \quad (28)$$

Equating these timescales and substituting $\nu_h \sim l_h v_h$ for the turbulent diffusivity, we indeed find $v_h \sim \Delta v$.

But this line of argument is naïve for several reasons. First, in the strongly stratified, quasi-2D flow in the tachocline the main mechanism of dissipation is not the nonlinear transfer between 2D modes but the viscous dissipation (due to overturning small-scale 3D turbulence) between neighbouring slabs. Thus, the dissipation timescale is rather

$$\tau_d \sim l_c^2/\nu. \quad (29)$$

Nevertheless, substituting here the formula (7), derived assuming the validity of equations (5) and (6), the result is again $v_h \sim \Delta v$, confirming that our assumption was consistent.

Secondly, equation (27) may not be a valid expression of the growth timescale if the instability is only slightly supercritical. Linear 2D hydrodynamical stability analysis indeed shows that the horizontal shear in the tachocline is close to marginal stability (Dziembowski and Kozovichev, 1987, Charbonneau, Dikpati, and Gilman, 1999). The weakly nonlinear extension of the analysis (Garaud, 2001b) indicates that the evolution of unstable modes is such that they modify the mean shear profile towards increasing stability, thus ensuring marginal stability, low growth rates and low velocity amplitudes. As, however, 3D effects and magnetic fields are known to lead to strong instability with much weaker shear (Gilman and Dikpati, 2000, Dikpati and Gilman, 2001), one may expect that this near-criticality is a feature limited to 2D HD models only.

Somewhat surprisingly, the 3D thin shell simulations of Miesch (2002) also show rather low nonaxisymmetric horizontal flow amplitudes, at least one order of magnitude below the shear amplitude. This is so despite the strongly supercritical rotation profile chosen, which is not significantly altered by the feedback of the nonaxisymmetric flow. One

may speculate that this is the result of the rather high numerical viscosities applied.

Further study of the flows driven by the horizontal shear instability is clearly important. In addition to clarifying the issue of characteristic scales of this flow, such studies may shed more light on the question of the importance and sense of any direct angular momentum transport by these motions. At any rate, a lower velocity amplitude or a longer timescale for the horizontal flows would result in lower critical field strengths for the secondary shear instability, resulting in an even thinner tachocline confined by even weaker fields in the framework of the present model.

4.2. OTHER SOURCES OF TURBULENCE

Another important constraint in the present model was the assumption that the secondary shear instability is the only source of turbulence in the tachocline. While a number of other instabilities in rotating radiative stellar interiors are known (cf. Tassoul, 1978, Zahn, 1983, Spruit, 1999), they are mostly acting throughout the radiative interior where constraints such as chemical mixing in stellar models impose rather strict limits on turbulence. Thus, in the tachocline we need “extra” sources of turbulence, for which shear instabilities are the most plausible candidate.

More important than rotational instabilities is the possibility of nonadiabatic overshooting convection. The recent solution of the Reynolds moment equations for the overshoot layer by Marik and Petrovay (2003) indicates that the total extent of nonadiabatic overshoot is negligible. On the other hand, Xiong and Deng (2001) find a very significant nonadiabatic overshoot. As both models have their own shortcomings, this issue is not quite settled yet. At any rate, if there is a significant nonadiabatic overshoot, the secondary shear instability would only set in below the overshoot layer, where the turbulent diffusivity is reduced below the critical value; in this layer, our model could still be considered valid. Thus, the main effect of any nonadiabatic overshoot would be to “shift” the resulting tachocline to somewhat lower depths (unless a stronger dynamo field reduces the horizontal shear already in the overshoot region).

5. Conclusion

This paper presented the first consistent model for the turbulent tachocline, with the turbulent diffusivity computed within the model instead

of being specified arbitrarily. For the origin of the 3D turbulence a new mechanism was proposed, the secondary vertical shear instability of 2D motions taking place in thin horizontal slabs.

Independent evidence for the mechanism proposed here is hard to find, as the conditions in the tachocline are extreme by terrestrial standards, and direct numerical simulations of stratified shear flows are currently limited to much lower values of the Richardson and Reynolds numbers. Nevertheless, the presence of a quasi-2D, layered structure, and a strongly anisotropic turbulent diffusivity tensor have been confirmed in numerical simulations by Métais and Herring (1989), Kaltenbach, Gerz, and Schumann (1994) and Jacobitz and Sarkar (1998). Indications for the presence of a secondary shear instability were also found in the recent simulations of Werne and Fritts (1999).

A formula for the diffusivity due to the turbulence generated by the secondary shear, equation (9) was derived and applied in a simple 1D model of the tachocline, taking into account the Maxwell stresses due to the dynamo field. As our analysis does not consider the effects of spherical geometry, rotation, non-adiabatic convective overshoot, meridional circulation, or the effect of magnetic fields on stability, it should only be regarded as a first step towards a more comprehensive theoretical analysis of the problem of turbulence in the solar tachocline.

A thin tachocline in our models can only be produced if the oscillatory dynamo magnetic field exceeds a critical limit. At this limit, the thickness of the tachocline is ~ 5 Mm and the mean value of the field strength in the tachocline is 200 G. The total magnetic flux in the tachocline in this case agrees well with the total poloidal flux crossing the equatorial plane in the poloidal flux transport model of Petrovay and Szakály (1999).

On the other hand, the tachocline resulting from our model is uncomfortably thin when compared to helioseismic constraints. Existing seismic calibrations of tachocline thickness (Basu and Antia, 2001) indicate a significantly thicker shear layer. These calibrations are based on the use of simple predefined fitting profiles, characterized by a single length scale. In contrast, our model indicates that for slightly subcritical magnetic field strengths the profile is more complicated, the fast linear cutoff in v within the skin layer being replaced by a shallow but deep profile of type (26) below. It remains to be seen, whether such a two-tiered v -profile can yield an equal or better fit to helioseismic data than the more conventional profiles.

The thin tachocline resulting from the present model is also hard to reconcile with the gradual depletion of lithium in the atmospheres of Sun-like stars during their lifetimes. Lithium is destroyed by nuclear reactions in layers below $z \sim 40$ Mm only, so a mixing characterized

by a diffusivity of at least $10^3 \text{ cm}^2/\text{s}$ must be present as far down as that depth. While our prescription $\nu_m = 10^7 \text{ cm}^2/\text{s}$ does not allow a firm statement on this issue, the very sharp cutoff of the ν -curve in the right-hand column of Fig. 2 does not seem to indicate that any significant level of turbulence could be maintained at such great depths. The two-tiered character of our profiles might admit some “leakage” of turbulence into much deeper layers, but this would imply some rather implausible fine-tuning of the dynamo field strength.

One obvious shortcoming of the present models is their simplified treatment of the time development and of the geometry. The development of more realistic, axially symmetric spherical models employing the viscosity formula (9) is in progress.

Acknowledgements

I am grateful for the hospitality of the Center for Turbulence Research at NASA Ames Research Center during part of this work. This paper owes much to discussions with A. Kosovichev, N. Mansour, M. Miesch and A. Wray. This work was supported by the OTKA under grants no. T032462 and T034998.

References

Basu, S. and Antia, H. M.: 2001, *Monthly Notices Roy. Astron. Soc.* **324**, 498
 Cally, P. S.: 2001, *Solar Phys.* **199**, 231
 Charbonneau, P., Dikpati, M., and Gilman, P. A.: 1999, *Astrophys. J.* **526**, 523
 Dikpati, M. and Gilman, P. A.: 2001, *Astrophys. J.* **551**, 536
 Dziembowski, W. and Kosovichev, A.: 1987, *Acta Astr.* **37**, 341
 Forgács-Dajka, E.: 2003, *Astron. Astrophys.* submitted,
 Forgács-Dajka, E. and Petrovay, K.: 2001, *Solar Phys.* **203**, 195
 Forgács-Dajka, E. and Petrovay, K.: 2002, *Astron. Astrophys.* **389**, 629
 Garaud, P.: 2001a, *Monthly Notices Roy. Astron. Soc.* **329**, 1
 Garaud, P.: 2001b, *Monthly Notices Roy. Astron. Soc.* **324**, 68
 Gilman, P. A. and Dikpati, M.: 2000, *Astrophys. J.* **528**, 552
 Gough, D. O. and McIntyre, M. E.: 1998, *Nature* **394**, 755
 Hopfinger, E. J.: 1987, *J. Geophys. Res.* **92**, 5287
 Jacobitz, F. G. and Sarkar, S.: 1998, *Phys. Fluids* **10**, 1158
 Kaltenbach, H.-J., Gerz, T., and Schumann, U.: 1994, *J. Fluid Mech.* **280**, 1
 Kosovichev, A. G.: 1996, *Astrophys. J.* **469**, L61
 MacGregor, K. B. and Charbonneau, P.: 1999, *Astrophys. J.* **519**, 911
 Marik, D. and Petrovay, K.: 2003, *Astron. Astrophys.* **396**, 1011
 Métais, O. and Herring, J. R.: 1989, *J. Fluid Mech.* **202**, 117
 Miesch, M. S.: 2001, *Astrophys. J.* **562**, 1058
 Miesch, M. S.: 2002, *Astrophys. J.* in press,

Petrovay, K.: 2000, in *The Solar Cycle and Terrestrial Climate*, ESA Publ. SP-463, p. 3

Petrovay, K. and Szakály, G.: 1999, *Solar Phys.* **185**, 1

Rüdiger, G. and Kitchatinov, L. L.: 1997, *Astr. Nachr.* **318**, 273

Speziale, C. G.: 1991, *Ann. Rev. Fluid Mech.* **23**, 107

Spiegel, E. A. and Zahn, J.-P.: 1992, *Astron. Astrophys.* **265**, 106

Spruit, H. C.: 1999, *Astron. Astrophys.* **349**, 189

Tassoul, J.-L.: 1978, *Theory of Rotating Stars*, Princeton UP

Thorpe, S. A.: 1987, *J. Geophys. Res.* **92**, 5231

Werne, J. and Fritts, D. C.: 1999, *Geophys. Res. Lett.* **26**, 439

Xiong, D. R. and Deng, L.: 2001, *Monthly Notices Roy. Astron. Soc.* **327**, 1137

Zahn, J.-P.: 1983, in A. N. Cox et al. (ed.), *Astrophysical Processes in Upper Main Sequence Stars*, Proc. Saas-Fee Winter School, Geneva Obs., p. 225

Address for Offprints:

K. Petrovay
Eötvös University, Dept. of Astronomy
Budapest, Pf. 32, H-1518 Hungary
E-mail: kris@astro.elte.hu